Optical Performance of Carbon-Nanotube Electron Sources

Niels de Jonge,[1,*] Myriam Allioux,[1,†] Jim T. Oostveen,[1] Kenneth B. K. Teo,[2] and William I. Milne[2]
[1]*Philips Research, Professor Holstlaan 4, 5656 AA Eindhoven, The Netherlands*
[2]*Department of Engineering, University of Cambridge, Trumpington Street, Cambridge CB2 1PZ, United Kingdom*
(Received 10 January 2005; published 11 May 2005)

The figure of merit for the electron optical performance of carbon-nanotube (CNT) electron sources is presented. This figure is given by the relation between the reduced brightness and the energy spread in the region of stable emission. It is shown experimentally that a CNT electron source exhibits a highly stable emission process that follows the Fowler-Nordheim theory for field emission, fixing the relationship among the energy spread, the current, and the radius. The performance of the CNT emitter under realistic operating conditions is compared with state-of-the-art electron point sources. It is demonstrated that the reduced brightness is a function of the tunneling parameter, a measure of the energy spread at low temperatures, only, independent of the geometry of the emitter.

DOI: 10.1103/PhysRevLett.94.186807 PACS numbers: 73.63.Fg, 29.25.Bx, 79.70.+q, 81.05.Tp

Individual carbon nanotubes (CNTs) can be used as point sources of electrons with extremely high brightness [1]. The energy spread of the emitted electron beam is typically on the order of 0.3 eV [2–4] for low currents and temperatures. Furthermore, when the emitting tip of the CNT is closed, the emission current can be highly stable [5,6]. The present status of the research on CNT electron sources was recently summarized [7]. But despite many reports, the figure of merit for the electron optical performance of CNT electron point sources has not yet been determined. This figure is the relation between the brightness and the energy spread for the current region of stable emission. The measurement of just one of these two parameters has a limited use as high brightness is usually obtained at the expense of an increased energy spread, adversely affecting the performance of the source in an electron optical system. In this Letter we present the figure of merit of the CNT electron source, derive a new model for this figure, and discuss its general applicability.

A series of measurements is presented on several multiwalled CNTs obtained from two different growth techniques, namely, arc discharge [8] and chemical vapor deposition (CVD) [9]. For precise characterization individual CNTs were mounted on tungsten support tips using a nanomanipulator system in a scanning electron microscope (SEM). Closed end caps were obtained for small diameter CNTs [6]. As the final step in the preparation the CNT electron source was cleaned by heating in an ultrahigh vacuum system (10^{-10} Torr). Each CNT was verified as having a closed cap and being cleaned by recording its field emission pattern [6,10]. The samples were heated to a temperature of at least 600 K during the emission experiments to remove volatile species continuously and to maintain a clean emission surface.

The stability of the emitted current of a carbon-nanotube electron source was tested by operating it at a constant voltage provided by a high-stability power supply and measuring the probe current I_p in a Faraday cup. Figure 1(a) shows that I_p has a maximal drift of 0.5% over 1 h. Fast Fourier transformation of the root mean square (rms) of I_p was performed with a spectrum analyzer to obtain the normalized spectral density $S_n(f) = \Delta I_p^2/I_p^2\Delta f$; see Fig. 1(b). A fit showed that $S_n \propto f^{-1}$ up to 25 Hz. It is expected that the signal will be limited at higher frequencies by shot noise $S_{n,\mathrm{shot}}(f) = 2e/I_p = 1.3 \times 10^{-10}$ Hz^{-1}. Integration leads to the rms noise percentage $np = \langle \Delta I_p^2 \rangle^{1/2}/I_p = 0.02\%$, a measure for the inverse signal-to-noise ratio. This value is extremely low for a cold field emitter, having typically 2%–3% fluctuations of I_p without a feedback system [11,12]. It is even smaller than the value of 0.2% for the Schottky emitter [12,13]. Table I shows small values of np for three other nanotubes as well. These findings demonstrate that an individual CNT with a closed cap and a cleaned surface behaves as a highly stable electron source, as expected on the basis of its rigid structure [7].

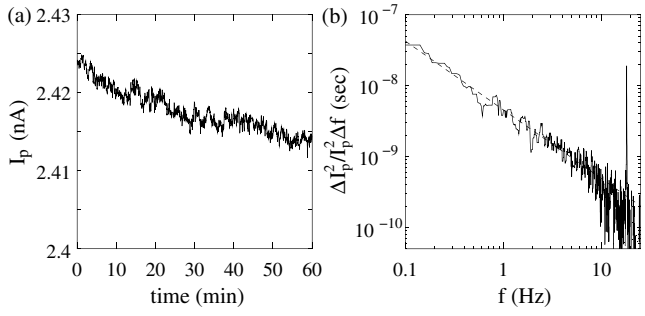

FIG. 1. Emission stability of electron source CNT 1. (a) The probe current I_p was measured as a function of time for a total emitted current of 200 nA, an extraction voltage of 270 V, and a temperature of 600 K. (b) The normalized spectral density as a function of the frequency f. The spectrum was corrected for the noise background of the measuring system. The dashed line is a fit with the function $y = a/x^{0.97}$.

TABLE I. Measurements of $I-U$ curves of CNT electron emitters, np measured at 100 nA in the range 0.1–25 Hz, β and R derived from the FN plot, and I_r' at 100 nA. CNT 2 was obtained by arc discharge, the others by CVD.

CNT	np	β (m^{-1})	R (nm)	ϕ (eV)	r_v (nm)	I_r' (nA/sr V)
1	0.02%	2.3×10^7	0.98	5.1	···	3.4
2	0.1%	1.7×10^7	0.59	5.1	···	2.1
3	···	8.1×10^6	4.6	5.1	···	2.1
4	0.2%	2.0×10^7	0.81	5.1	···	1.9
5	···	1.2×10^7	1.5	5.4	···	1.4
6	···	7.4×10^6	3.0	···	1.8	5.3
7	···	1.6×10^7	1.7	···	1.6	2.5
8	0.2%	2.1×10^7	1.7	···	1.7	4.0

The electron emission of a cleaned CNT with a closed cap is caused by field emission with a work function of 5.1 ± 0.1 eV [3,14]. The current density J follows the Fowler-Nordheim (FN) theory [15], which can be expressed as [3,14–16]

$$J = c_1\frac{F^2}{b_1^2\phi}\exp\left\{a_2c_2c_3\frac{1}{\sqrt{\phi}}\right\}\exp\left\{-a_1c_2\frac{\phi^{3/2}}{F}\right\} \quad (1)$$

with work function ϕ and electric field F. The constants are defined as $a_1=0.958$, $a_2=1.05$, $b_1=1.05$, $c_1=e^3/8\pi h$ with the electron charge e and Planck's constant h, $c_2=8\pi\sqrt{2m}/3he$ with electron mass m, and $c_3=e^3/4\pi\epsilon_0$ with the permittivity of free space ϵ_0. The total current is given by

$$I = 2\pi R^2 J, \quad (2)$$

assuming a hemispherical emitting surface with a radius of curvature R. The local field at the apex of a sharp electrically conducting tip equals the product of the extraction voltage U and the field enhancement factor β, which can be computed numerically knowing the geometry of the emitter. A graph of $\log I/U^2$ versus $1/U$, the FN plot, is thus a linear curve.

The current-voltage characteristics were recorded for eight CNTs. All FN plots were linear, indicating that field emission was occurring for all CNTs. Values of β were obtained from the slopes of the FN plots, and values of R were derived from the point at which $1/U$ was zero. The results are shown in Table I. Transmission electron microscopy (TEM) images of the CNT batch sample and of several mounted CNTs revealed that most CNTs had a few walls and a radius between 1 and 3 nm, consistent with the values obtained from the FN plots. A TEM image of CNT 1 taken after the emission measurements confirmed a radius of 1.1 nm. The values of the field enhancement factor are as expected on the basis of numerical calculations [14].

The current density as a function of the energy E is approximately proportional to [16]

$$J(E) \propto \frac{\exp(E/d)}{1+\exp(E/k_BT)}, \quad (3)$$

where k_B is the Boltzmann constant, T is the temperature, and d is the tunneling parameter, given by

$$d = \frac{c_4F}{b_1\sqrt{\phi}} \quad (4)$$

with $c_4=eh/4\pi\sqrt{2m}$. The total energy spread of the emitted electron beam is often expressed by the full width at half maximum of the energy spectrum ΔE. The width of the low-energy side of the energy spectrum is determined by d, while T sets the width of the high-energy side. ΔE can be approximated in the parameter range $100<T<1000$ K and $0.2<d<0.5$ eV as

$$\Delta E \cong 3.1\times10^{-4}T + 0.72d. \quad (5)$$

Energy spectra were recorded with a hemispherical energy analyzer for five CNTs at different currents (10–500 nA) and temperatures (500–900 K). A typical energy spectrum is shown in Fig. 2(a). These spectra were fitted to Eq. (3) to obtain values for d and T. Several spectra measured in the higher current regime contained significant shoulders at the low-energy side of the main peak. From these spectra values of d and T could still be determined in most cases, but values of ΔE were not extracted from these spectra. The values of ΔE were corrected for the resolution of the spectrometer.

The plot of d versus I of two CNTs with respective diameters of 0.6 and 4.6 nm is shown in Fig. 2(b). Numerically calculated curves [using Eqs. (1), (2), and (4)] of d versus I for both radii overlap well with the measurements showing that the data are consistent with the FN model. We can thus express d as a function of R and I only. Note that the value of d increases with decreasing R for a given I.

The data of the FN plot and the energy spectrum can be combined, in order to determine ϕ, using

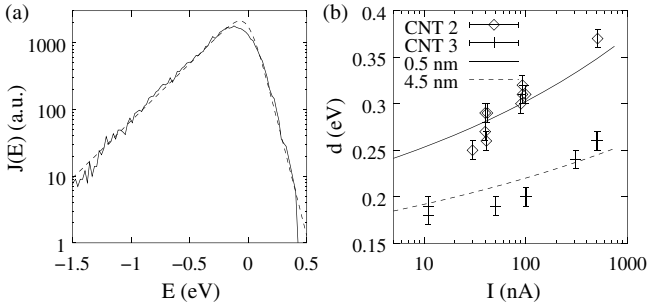

FIG. 2. (a) Energy spectrum of CNT 2 and fit with the FN theory (dashed line). (b) Tunneling parameter d as a function of I for two CNTs, compared with numerically calculated curves.

$\phi = -1.64bd/U$, with b the slope of the FN plot and U the extraction voltage at which the energy spectrum was measured [3,14]. The obtained values are indicated in Table I alongside each CNT and are consistent with the expected value of 5.0 eV.

The most important parameter of an electron source is its brightness. Usually the brightness is normalized on U, the electron energy at which the brightness is measured, thus obtaining the reduced brightness B_r [16]:

$$B_r = \frac{dI}{d\Omega}\frac{1}{\pi r_v^2}\frac{1}{U} = \frac{I_r'}{\pi r_v^2} \tag{6}$$

with the reduced angular current density I_r' and the radius of the virtual source r_v. For a focusing system with ideal lenses the reduced brightness indicates the amount of current, which can be focused into a spot of certain size and electron beam energy. Both I_r' and r_v were measured with, respectively, a Faraday cup and a point projection microscope, for several CNTs to obtain B_r. The method was described elsewhere [1,17]. I_r' was obtained for eight CNTs. The average value was 2.8 nA/sr V at $I = 100$ nA (see Table I). Measurements at other current levels revealed approximately a linear relationship between I_r' and I. As can be seen from Fig. 3, $I_r'/I_{r,100\,\mathrm{nA}}' = 0.25 + 0.0073 \times I/\mathrm{nA}$. Within a factor of 2 accuracy I_r' can now be expressed by

$$I_r' \cong 0.0073 \times 2.8 \times I/\mathrm{sr\,V} = 0.02 \times I/\mathrm{sr\,V}. \tag{7}$$

The virtual source sizes of three CNTs were measured; two were found to be almost equal to R and one was a factor of 1.7 smaller; see Table I. Thus, for CNTs with small radii,

$$r_v \cong R. \tag{8}$$

This observation is consistent with previous conclusions [17].

Using the relations (7) and (8) and recognizing that d is a function of F and ϕ, the brightness can be rewritten within a factor of 3 accuracy as

$$B_r \cong \frac{0.02I}{\pi R^2} = 0.04J(F, \phi) = 0.04J(d, \phi). \tag{9}$$

Since ϕ is constant for a certain material, Eq. (9) shows that B_r is a function of d only. Figure 4 shows the data obtained for five CNTs and a plot of Eq. (9). The data correspond well with the theory. An important aspect of Eq. (9) is that it is independent of the actual shape of the CNT, expressed in R, its length l, and other geometrical factors, such as the geometry of the surrounding electrodes. This can be explained as follows. A thin CNT results in a relatively large value of d (as shown in Fig. 2) but, on the other hand, has a small value of r_v and a corresponding large brightness and vice versa for a thicker CNT.

Our systematic study shows that it is now possible to select the optimal CNT electron point source from CNTs with a range of diameters and lengths, as the relation between B_r and d, determining the optical performance of the source, does not depend on these parameters. We expect that our result of Eq. (9) is more generally applicable to field emitters of nanometer size, for example, nanometer-sized tungsten tips and metallic nanowires. The upper and lower limits are set by the minimal current required for sufficient signal to noise in the application (e.g., imaging) and the maximum current at which the emitter can still operate properly. A further restriction is that the vibration amplitude of the CNT, expressed as the ratio R^4/l^3, should be kept sufficiently small [18]. It is important to notice that the determination of the brightness, which is often a complicated experimental procedure, is reduced to recording a FN plot and measuring I_r'.

In the 1960s, an expression was derived for the maximum theoretical brightness of a field emitter [19]:

$$B_r = Je/\pi d. \tag{10}$$

This equation predicts dependence on d and ϕ as well, but

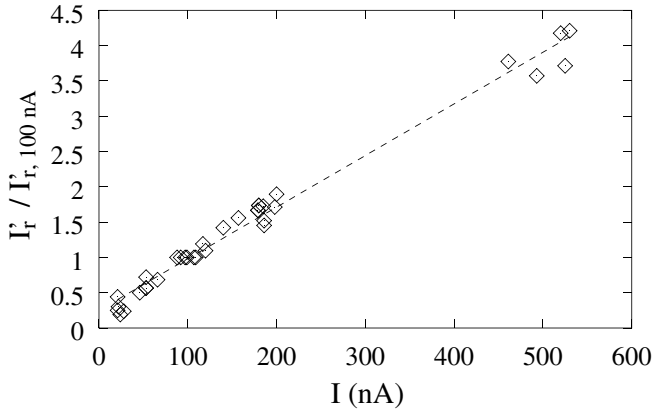

FIG. 3. Reduced angular current density I_r' normalized on I_r' at 100 nA for 8 CNT electron sources and a linear fit (dashed line).

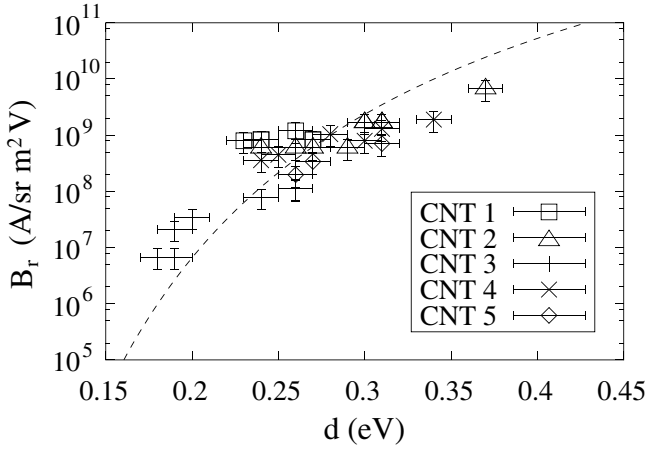

FIG. 4. Reduced brightness B_r as a function of the tunneling parameter d measured for 5 CNTs and compared with the calculated curve using $B_r = 0.04 \times J(d, \phi = 5.0\ \mathrm{eV})$ (dashed line).

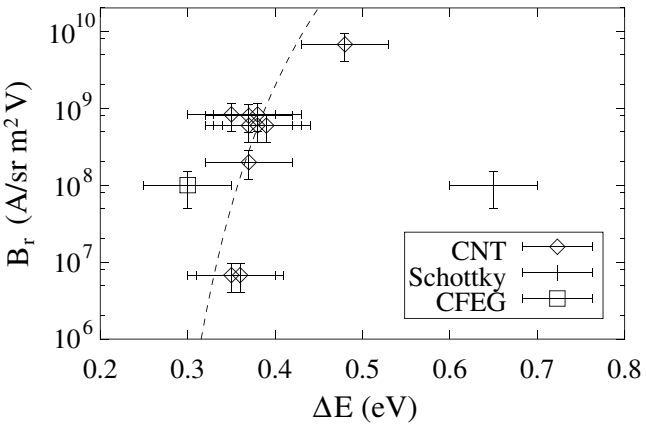

FIG. 5. B_r as a function of ΔE measured for several CNTs at currents of 10–500 nA and temperatures of 600–700 K. Calculated curve (dashed line). The data of the Schottky emitter and the CFEG are also included.

its value is typically a factor of 15 to 30 larger than Eq. (9). This difference is explained as follows. Typical field emitters consisting of a metal tip with a hemispherical emitting surface with $R > 50$ nm have a much smaller value of r_v than R [16]. For CNTs, on the contrary, $r_v \cong R$ [17]. Others found $r_v \cong 0.5R$ for nanometer-sized tungsten electron sources [20]. Thus, r_v approaches R when the emitting surface is reduced towards a few nanometers and deviates in shape from hemispherical. Furthermore, the broadening effect of Coulomb interactions [21] was not accounted for in Eq. (10).

At room temperature and at low currents d is almost equal to ΔE, and therefore Fig. 4 presents the figure of merit of the CNT electron source. However, some heating to 500–800 K was required to obtain stable emission, which broadens the energy spectrum. A secondary effect is that Joule heating at larger currents also leads to a broadening of the energy spectrum [22]. The figure of merit of electron sources under realistic conditions, B_r versus ΔE, is presented in Fig. 5. The curve was calculated using Eqs. (1), (2), (4), and (5). For comparison, data of state-of-the-art electron sources, the tungsten cold field emission gun (CFEG) [11], and the Schottky emitter [13] are included. Being cold field emitters, the CNT and the CFEG have an almost identical ΔE. However, the CFEG often lacks emission stability [11], which the CNT clearly has, as shown in Fig. 1. Note also that the CNT has a much higher B_r than the CFEG at high currents. Our values imply a significant improvement with respect to the Schottky emitter, either a lower ΔE at similar B_r or a much higher B_r at similar ΔE. Future research might aim to find nanomaterials with similar strength as CNTs, but with an intrinsically lower ϕ, which directly leads to an improvement of the figure of merit. Possibly, CNTs with larger radii than used in this experiment and with hemispherical cap shapes may improve the figure of merit as well.

In conclusion, CNT electron sources exhibit a highly stable emission that follows the Fowler-Nordheim theory of field emission, thus predicting the energy spread for a given current, radius, and temperature. The optical performance of the CNT under realistic conditions is a clear improvement with respect to state-of-the-art electron point sources. Its reduced brightness can be expressed as function of the tunneling parameter only, and hence the resultant figure of merit is independent of the geometry of the emitter.

The authors thank M. Doytcheva, M. Kaiser, R. Lacerda, S. A. M. Mentink, A. G. Rinzler, T. van Rooij, G. Schwind, A. S. Teh, and G. van Veen. This work was supported by FEI company, the EC, the EPSRC, and the Dutch Ministry of Economic Affairs.

*Present address: Oak Ridge National Laboratory, Oak Ridge, TN 37831, USA.
Electronic address: dejongen@ornl.gov
†Present address: ESPCI Paris, 10 Rue Vauquelin, 75005 Paris, France.

[1] N. de Jonge, Y. Lamy, K. Schoots, and T. H. Oosterkamp, Nature (London) **420**, 393 (2002).
[2] J. M. Bonard *et al.*, Appl. Phys. A **69**, 245 (1999).
[3] O. Groening *et al.*, J. Vac. Sci. Technol. B **18**, 665 (2000).
[4] A. Takakura *et al.*, Ultramicroscopy **95**, 139 (2003).
[5] A. G. Rinzler *et al.*, Science **269**, 1550 (1995).
[6] N. de Jonge *et al.*, Adv. Mater. (to be published).
[7] N. de Jonge and J. M. Bonard, Phil. Trans. R. Soc. A **362**, 2239 (2004).
[8] D. T. Colbert *et al.*, Science **266**, 1218 (1994).
[9] R. G. Lacerda *et al.*, Appl. Phys. Lett. **84**, 269 (2004).
[10] K. A. Dean and B. R. Chalamala, J. Vac. Sci. Technol. B **21**, 868 (2003).
[11] J. F. Hainfeld, Scanning Electron Microsc. **1**, 591 (1977).
[12] D. Tuggle, L. W. Swanson, and J. Orloff, J. Vac. Sci. Technol. **16**, 1699 (1979).
[13] L. W. Swanson and G. A. Schwind, in *Handbook of Charged Particle Optics*, edited by J. Orloff (CRC Press, New York, 1997).
[14] N. de Jonge *et al.*, Appl. Phys. Lett. **85**, 1607 (2004).
[15] R. H. Fowler and L. Nordheim, Proc. R. Soc. A **119**, 173 (1928).
[16] P. W. Hawkes and E. Kasper, *Principles of Electron Optics II: Applied Geometrical Optics* (Academic Press, London, 1996).
[17] N. de Jonge, J. Appl. Phys. **95**, 673 (2004).
[18] J. H. Hafner, L. C. Chin, T. H. Oosterkamp, and C. M. Lieber, J. Phys. Chem. B **105**, 743 (2001).
[19] J. Worster, Br. J. Appl. Phys. **2**, 457 (1969).
[20] W. Qian, M. R. Scheinfein, and J. C. H. Spence, J. Appl. Phys. **73**, 7041 (1993).
[21] P. Kruit and G. H. Jansen, in *Handbook of Charged Particle Optics* (Ref. [13]).
[22] S. T. Purcell, P. Vincent, C. Journet, and V. ThienBinh, Phys. Rev. Lett. **88**, 105502 (2002).